NASA TECHNICAL MEMORANDUM

NASA TM X-73958

FLIGHT DATA IDENTIFICATION OF SIX DEGREE-OF-FREEDOM STABILITY AND CONTROL DERIVATIVES OF A LARGE "CRANE" TYPE HELICOPTER

Robert L. Tomaine
Langley Directorate
U.S. Army Air Mobility R&D Laboratory
NASA-Langley Research Center
Hampton, Virginia 23665

National Aeronautics and Space Administration

Langley Research Center
Hampton, Virginia 23665

1. Report No.	2. Government Accession No.	3. Recipient's Catalog No.
NASA TM X-73958		

4. Title and Subtitle	5. Report Date
Flight Data Identification of Six Degree-of-Freedom Stability and Control Derivatives of a Large "Crane" Type Helicopter	September 1976
	6. Performing Organization Code
7 Author(s)	8. Performing Organization Report No.
Robert L. Tomaine	
	10. Work Unit No.
9 Performing Organization Name and Address	
NASA-Langley Research Center Hampton, VA 23665	11 Contract or Grant No.
	13 Type of Report and Period Covered
12 Sponsoring Agency Name and Address	Technical Memorandum
National Aeronautics and Space Administration Washington, DC 20546	14 Sponsoring Agency Code

15. Supplementary Notes

The research effort which has lead to the results in this report was financially supported by USAAMRDL (Langley Directorate).

16 Abstract

Flight test data from a large "crane" type helicopter was collected and processed for the purpose of identifying vehicle rigid body stability and control derivatives. The process consisted of using digital and Kalman filtering techniques for state estimation and Extended Kalman filtering for parameter identification utilizing a least squares algorithm for initial derivative and variance estimates. Data was processed for indicated airspeeds from 0 m/sec to 152 m/sec (90 knots). Pulse, doublet and step control inputs were investigated. Digital filter frequency did not have a major effect on the identification process, while the initial derivative estimates and the estimated variances had an appreciable effect on many derivative estimates. The major derivatives identified agreed fairly well with analytical predications and engineering experience. The derivative identification process produced very inconsistent results for non-major derivatives.

The use of predicted derivative uncertainty was found to be inadequate for assessing identification accuracy and flight data regeneration (data used in the reconstruction of identification process) results were found to be inconsistent with flight simulation (prediction of data not used in identification process) results. Doublet control inputs provided better results than pulse or step inputs.

17. Key Words (Suggested by Author(s))	18 Distribution Statement
Parameter identification VTOL stability derivatives Extended Kalman filtering	Unclassified - Unlimited

19. Security Classif. (of this report)	20. Security Classif (of this page)	21 No. of Pages	22 Price*
Unclassified	Unclassified	55	$4.25

* For sale by the National Technical Information Service, Springfield Virginia 22161

FLIGHT DATA IDENTIFICATION OF SIX DEGREE-OF-FREEDOM STABILITY AND CONTROL DERIVATIVES OF A LARGE "CRANE" TYPE HELICOPTER

Robert L. Tomaine
Langley Directorate, U.S. Army Air Mobility R&D Laboratory

SUMMARY

An advanced parameter identification process was used to identify six degree-of-freedom rigid body stability and control derivatives from flight test measurements for a large "crane" type helicopter. Data was processed for a range of airspeeds and for pulse, step and doublet control inputs. The sensitivity of the identification results to processing parameters was investigated. The acceptability of the identified derivatives was examined using data regeneration and simulation, comparison with analytical results and using engineering judgment.

The identified major derivatives agreed reasonably well with analytical results and intuitive engineering analysis. The non-major derivatives identified were inconsistent. The doublet input data provided superior results to the step and pulse input data.

INTRODUCTION

There are several existing techniques for determining values of stability and control derivatives for a fixed wing vehicle. They include

wind tunnel testing, semiempirical methods such as U.S.A.F. DATCOM and Royal Aeronautical Society Data Sheets, and flight-test identification methods (see Ref. 1). Wind tunnel testing can provide good estimates for static derivatives (e.g., functions of α and β) but has limitation for providing dynamic derivatives (e.g., associated with velocities or rates). Semiempirical methods which utilize aircraft geometry and aerodynamic characteristics have been used to provide preliminary design derivative values but are limited in accuracy and may not provide acceptable estimates for a new configuration. Semiempirical methods have not been developed for helicopter configurations and the same fixed wing limitations for wind tunnel testing exists for helicopters in addition to requiring more sophisticated models and rotor dynamic scaling. The third method, while existing for many years, has not enjoyed large success in fixed wing application and has only recently been employed for helicopter application (see Ref. 2, 3, 4). The method of determining stability derivatives from flight-test measurements of vehicle and control states is commonly known as "stability derivative extraction" and is a form of parameter identification. The general procedure for extracting stability derivatives from flight data is to form a small perturbation mathematical model of the aircraft equations of motion, provide measurements of the vehicle states, and solve for the coefficients in the aerodynamic portion of the model. In vector notation the governing sets of equations are:

$$\dot{\bar{X}} = A\bar{X} + B\bar{u}$$

where $\bar{X}$ contains the vehicle state variables, $\bar{u}$ the control system state

variables, A contains the stability derivatives, and B contains the control derivatives. The procedure is to solve for the components of A and B given measurements of $\bar{X}$, $\dot{\bar{X}}$, and $\bar{u}$.

SYMBOLS

Values are given in both SI and U.S. Customary Units. The measurements and calculations were made in U.S. Customary Units.

A_{ls}	lateral cyclic control angle, deg.
A/S	indicated airspeed, m/sec (knots)
B_{ls}	longitudinal cyclic control angle, deg.
f_c	digital filter cutoff frequency, hertz
f_t	digital filter termination frequency, hertz
g	acceleration due to gravity, m/sec^2 (ft/sec^2)
G	process noise gain matrix
IAS	indicated airspeed, m/sec (knots)
I_{xx}	vehicle rolling moment of inertia, kg-m^2 (slug-ft^2)
I_{xz}	vehicle product of inertia, kg-m^2 (slug-ft^2)
I_{yy}	vehicle pitching moment of inertia, kg-m^2 (slug-ft^2)
I_{zz}	vehicle yawing moment of inertia, kg-m^2 (slug-ft^2)
L	total rolling moment, m-N (ft-lbs)
M	total pitching moment, m-N (ft-lbs)
$\bar{n}$	white gaussian measurement noise vector

N	total yawing moment, m-N (ft-lbs)
p	vehicle roll rate, rad/sec
P_{11}	state variable covariance matrix
P_{p_1}	cross covariance matrix
q	vehicle pitch rate, rad/sec
r	vehicle yaw rate, rad/sec
u	X axis velocity component, m/sec (ft/sec)
v	Y axis velocity component, m/sec (ft/sec)
w	Z axis velocity component, m/sec (ft/sec)
$\bar{w}$	zero mean white gaussian process noise
X	total longitudinal force, N(lbs)
$\bar{X}_p$	stability derivative vector
Y	total lateral force, N (lbs)
Z	total vertical force, N (lbs)
α	vehicle angle of attack, rad.
ϕ	vehicle roll angle, deg.
β	vehicle sideslip angle, rad.
θ	vehicle pitch attitude, deg.
ψ	vehicle yaw attitude, deg.
θ_{TR}	tail rotor collective pitch at blade root, deg.
θ_{MR}	main rotor collective pitch at blade root, deg.
ζ	designates control input perturbation
σ	derivative uncertainty, derivative units
σ^2	derivative variance, derivative units squared

Subscripts

o Refers to initial trim condition.

Superscripts

A dot refers to first derivative with respect to time (e.g., $\dot{u} = \frac{\partial u}{\partial t}$)

A bar refers to a vector quantity.

Derivatives

Derivatives are normalized by mass or inertia. Derivative units are determined by force or moment units divided by appropriate state variable unit and mass or inertia, e.g. M_q, 1/sec.

$$\frac{\text{ft - lbs}}{\text{rad/sec - slug - ft}^2} \cdot \frac{\text{ft slug}}{\text{lb sec}^2} = 1/\text{sec}$$

Derivative Notation

A shorthand derivative notation is used to simplify derivative expressions as illustrated by the following example:

$$\frac{\partial L}{\partial A_{1s}} \equiv L_{A_{1s}}$$

In addition, four derivatives contain inertial terms and are defined as follows:

$$X_q = \frac{\partial X}{\partial q} - w_0,\ Y_p = \frac{\partial Y}{\partial p} + w_0,\ Y_r = \frac{\partial Y}{\partial r} - u_0,\ Z_q = \frac{\partial Z}{\partial q} + u_0$$

Symbols Used on Computer Plots

THETA COLL	main rotor collective pitch angle, deg.
THETA TAIL	tail rotor collective pitch angle, deg.
1 SIGMA	derivative uncertainty (1 σ), derivative units

BACKGROUND

As previously stated, extraction of stability derivatives from flight-test measurements for fixed wing vehicles is not a new idea. Documented results (see Ref. 1) are found as early as 1925. Two of the predominant early methods were analog matching and least-squares curve-fitting techniques. Both methods have yielded some success in identifying primary derivatives and associated characteristic modes for uncoupled longitudinal or lateral-directional models. Applications of these early methods provided a basis for development of advanced extraction techniques and have resulted in the identification of several inherent problems associated with estimation of stability and control derivatives from applications of flight-test measurement techniques. Some of these problems are associated with the assumptions necessary to establish a mathematical model of the vehicle and others are associated with the limitations and complications of in-flight measurement of state variables. The major problems involving the mathematical model are: (1) exclusion of terms which have non-negligible values, (2) lack of provisions for nonlinear aerodynamics, (3) exclusion of coupling (longitudinal and lateral-directional) effects, (4) accounting for random disturbances (wind gusts, etc.) and (5) lack of modeling higher

degrees of freedom. These errors are generally categorized as sources of process noise. Another inherent problem of the mathematical model is that there are more derivatives to be identified than there are independent equations such that the solution (estimated derivatives) is nonunique. In addition, since the equations of motion are written about an equilibrium condition, the failure to precisely trim the vehicle introduces an error source.

The problems associated with state variable measurements are: (1) inaccuracy of physical transducers used to evaluate the variables, (2) errors introduced by filtering (recording, reducing, and preprocessing data), (3) measurement bias errors due to drift or calibration errors, (4) misalignment and instrumentation uncertainty, and (5) noise due to aircraft vibration, physical transducers, or recording system.

In addition to these major categories of error sources, the choice of pilot input has been shown to be an important consideration. Thus, all three areas must be considered before successful derivative extraction from flight data is realized.

Three types of methods for parameter identification have been developed over the years for aircraft application. They are: (1) equation error methods such as classical least squares which minimize process noise effects, (2) output error methods such as Newton-Raphson and Kalman filter which minimize measurement noise effects, and (3) advanced statistical methods such as Maximum Likelihood and Extended Kalman filtering which account for both process and measurement noise (see Ref. 1). Since helicopter flight data contain substantial measurement and process noise, successful extraction

requires application of one of the advanced methods or at least a combination of high-quality data filters combined with an equation error method.

Since the helicopter stability derivative identification problem combines all of the previously mentioned problems, existing fixed wing analyses are not generally applicable. A parameter identification technique specifically designed for helicopter application (Ref. 2) has been applied to flight test data from a large "crane" type, articulated rotor helicopter. The method chosen, as described in Figure 1, consist of essentially four processes. Flight measured state variables are digitally filtered using a Graham high-quality, zero phase shift filter (see Ref. 5) with a very high roll-off rate. The purpose of the digital filter is to retain only rigid body frequency data. The digital filtered data is then processed twice through a Kalman filter, first to estimate measurement biases in the measured data set, and then to account for random discrepancies of related measurements and generally improve the quality of the data. The Kalman filter can also reproduce states for which data is not available, provided related data is available. The Kalman filtered data is then used in a least squares algorithm to provide initial derivative and variance estimates for initializing the Extended Kalman filter (Bayesian Maximum Likelihood Estimator, Ref. 2) algorithm for parameter identification. The least squares estimated variances are known to be conservative (Ref. 6) and are adjusted upward. The parameter identification algorithm used determines the most probable estimates of the state variable and stability derivatives given the measured data. The parameters to be identified (stability derivatives) along with the aircraft states are combined to

form an augmented state; the resulting state equation is nonlinear and an Extended Kalman filter is used to approximate an optimal nonlinear filter. The resulting system equations are:

$$\dot{\bar{X}}_i(t) = f(\bar{X}_i, \bar{X}_p) + G_i \bar{w}_i(t)$$

$$\dot{\bar{X}}_p = 0$$

where i represents the maneuver number, $\bar{X}_p$ represents the stability derivative vector, G is the process noise given matrix and $\bar{w}$ is zero mean white gaussian process noise. The measurement equations can be represented by: $Z_i = \bar{X}_i + \bar{n}_i$, where $\bar{n}$ is white gaussian measurement noise and Z the measured state variable. The estimates for the state variable and stability derivatives are obtained from the following filter equations:

$$\dot{\bar{X}} = f(\bar{X}, \bar{X}_p) + P_{11}R^{-1}(\bar{Z} - \bar{X})$$

$$\dot{\bar{X}}_p = P_{p1}R^{-1}(\bar{Z} - \bar{X})$$

where P_{11} and P_{p_1} are the state variable covariance matrix and the cross covariance matrix for the state and parameter vector and R is the measurement noise intensity matrix (see Ref. 2). The algorithm is programmed so that several data sets (maneuvers) can be processed simultaneously to minimize the effect of process noise.

The validity of the identified derivatives is then evaluated using several procedures. The identified derivatives are combined with the chosen math model and state variable time histories are generated using

the control inputs from the identification flight data (regenerated data). The Root Mean Square (RMS) error between the filtered flight data and the regenerated data is then computed. Time histories are also simulated using the identified derivatives and flight data control inputs not used in the identification process (simulated data) and RMS errors are calculated between the flight data and simulated data. The Extended Kalman filter algorithm estimates the derivative uncertainty (1 σ) for each derivative estimate. The relative magnitudes of the estimated uncertainty and the time history of the uncertainty can be used to judge the results of the derivative identification process. In addition, the derivatives and chosen model are used to compute the vehicle characteristic modes (e.g. eigenvalues). Comparison of the computed eigenvalues and the identified derivatives are made with available analytical results and engineering judgment is used to assess the acceptability of the id. tified derivatives.

Since the algorithm used has the capability to simultaneously process several maneuvers, data including all four pilot inputs can be used and a coupled six degree-of-freedom model can be identified. The aerodynamic portion of the model contains thirty-six stability derivatives and twenty-four control derivatives. The stability derivatives are first order Taylor series expansions for aerodynamic forces and moments for u, v, w, p, q, and r. The control derivatives are first order terms of longitudinal cyclic, lateral cyclic, tail rotor collective pitch and main rotor collective pitch. The equations representing the chosen model are given in Figure 2.

FLIGHT DATA

A flight test of the large "crane" type, articulated rotor helicopter shown in Figure 3, was performed to gather data for application of the stability derivative identification method previously described. The vehicle characteristics are given in Table 1. The vehicle was instrumented to provide data for airspeed, angles of attack and sideslip, vehicle attitude (Euler angles), rates, linear and angular accelerations and pilot control inputs. Data were sampled eighty-three times each second and recorded on magnetic tape. The vehicle was flown at a nominal gross weight of 128998.N (29,000 lbs) with center of gravity at 8.33m (328 inches). The test variables were airspeed and pilot control input shape. The test procedure required trimming the vehicle at a selected airspeed and then independently apply sequential control inputs of longitudinal stick, lateral stick, pedal movement and collective stick displacement while returning the vehicle to trim between successive control inputs. The matrix of test runs is shown in Table II.

RESULTS AND DISCUSSION

Procedure Variations

Several variations to the general identification procedure described previously were conducted in order to assess derivative sensitivity to the identification process. These included; variation of the digital filter cutoff and termination frequencies, adjustment of the least squares estimated derivative variances and modifications to the least squares initial derivative estimates.

Digital Filter

The purpose of digitally filtering the measured flight data is to remove high frequency data content to enhance rigid body derivative identification. A previous application of the method employed in this study to another flight vehicle (Ref. 2) was performed with an arbitrary digital filter cutoff and termination frequency. Analytical predictions (see Ref. 7) of the rigid body characteristic mode frequencies for this vehicle are all less than 1 hz. Flight data for this study was digitally filtered with cutoff frequencies of 1 hz, 2 hz, 3 hz, and 4 hz. The average RMS error between the regenerated and filtered flight data, the major derivative estimates and uncertainties were tabulated and compared in order to assess the effect of the filter frequency. The major derivative estimates and associated uncertainties are shown in Tables IV and V, respectively. The average derivative uncertainty did not appreciably change with filter frequency, but some major derivative values change substantially. At a cutoff frequency of 4 hz the major derivative estimates showed the largest variation indicating, that more consistent results would be obtained by processing data at lower than 4 hz cutoff frequencies. The digital filter cutoff and termination frequencies chosen determine the amount of high frequency rotor effects present in the filtered state variables and reduces the overall measurement noise content. Figure 4 shows a time history of vertical acceleration measurement to demonstrate the effect of the filter frequency on the measured state variables. The results shown in Tables III, IV and V indicate that the presence of high frequency data content did not measureably degrade the estimation process below 4 hz digital filter cutoff frequency.

Least Squares Variance

As previously stated the Extended Kalman filter algorithm used in this study requires estimates of initial derivative values and their variances. The least squares algorithm provides the initial derivative estimates and an estimate of the derivative variances which is known to be conservative. Therefore, the normal procedure is to multiply all the least squares estimated variances by a multiplication factor. Data were processed for five Least Square Variance Factors (LSQVF) ranging from 25 to 150. The RMS Errors between regenerated data and filtered data, major derivative estimates and uncertainties are tabulated in Tables VI through VIII, respectively. The RMS errors and derivative uncertainties suggest a good value for LSQVF is 100. Several derivative estimates, including Z_w and $Z_{\theta_{MR}}$, were very sensitive to the LSQVF.

Initial Derivative Estimate

The sensitivity of the derivative identification process to the initial derivative estimates was also investigated. The least squares derivative estimates were increased by fifty per cent and processed through the Extended Kalman filtering algorithm with a data set previously processed with the initial least square derivative estimates. The LSQVF for both runs was 100. The major derivative estimates for both data runs are shown in Table IX. Most of the final derivative estimates were within twenty-five per cent of the original final estimates. Several of the derivative estimates including the important derivative M_w, showed a marked increase. However,

the absolute value of M_w for this case was small and would not indicate a major change in predicted vehicle stability.

Pilot Input Shape

Flight data was obtained using three pilot input shapes. The data were processed in order to determine if there was any advantage in using a particular pilot input for identification among the three most common stability flight test inputs. This analysis was not an attempt to determine an optimum input (see Ref. 8 and 9), but was intended to provide an indication of the best data to be chosen from previous flight testing results. The three most common inputs used for stability and control testing are pulse, step and doublet inputs. A typical input of each type as used in this study is shown in Figure 5. Flight data for a nominal 60 KIAS case for each of the input shapes were processed, and the derivative estimates and uncertainties are shown in Tables X and XI. The RMS errors for regenerated and simulated data are shown in Table XII. The doublet input produced the lowest composite RMS errors for regeneration and simulation of other maneuvers. The derivative uncertainties were not a strong function of input shape. Examination of the derivative values shows that the predicted uncertainty was not a good indicator of accuracy since the derivatives estimated from data using step inputs are obviously in error, yet the predicted uncertainties are not high. For the step input run Z_q was estimated at -444.6 and $Z_{\theta_{TR}}$ AT 15.18. Both of these estimates are very high in comparison to all other results. The doublet input provides

the best results of the three shapes processed. This result is consistent with the intuitive reasoning that the doublet can provide good excitation while keeping the vehicle response within the linear assumptions of a small perturbation model.

Airspeed Variations

Data were obtained for indicated airspeeds of 0 m/sec (hover), 51 m/sec (30 knots), 101 m/sec (60 knots), and 152 m/sec (90 knots). Variations of the major derivative estimates with airspeed are shown in Table XIII. Also shown in Table XIII are derivatives predicted by a digital flight simulation computer program (see Ref. 7) for the subject vehicle at the same flight conditions. The derivative values agree fairly well with the exceptions of L_v, M_q, and N_p, and the control derivatives. The variation of identified derivatives with increasing airspeed also corresponds fairly well with the analytical computer program results.

Final Data Sets

Data were processed for the 101 m/sec (60 knots) flight condition for pulse and doublet inputs utilizing the results of the process sensitivity analysis. The LSQVF was set at 100 and the data was digitally filtered at 3 hz and 4 hz cutoff and termination frequencies, respectively. The results of this processing were analyzed using the following methods: examination of derivative values using engineering judgment and analytical predictions, RMS errors between regenerated data and filtered flight data

used in the identification process, RMS errors between simulated data and filtered flight data not used in the identification process, examination of estimated derivative variances and conversion characteristics and comparison of eigenvalues with analytical predictions. Since the rotor degrees-of-freedom are not modeled the estimated derivatives are a combination of the rigid body derivatives and average rotor contribution. Depending on the location of the rotor characteristic modes these derivatives may not be equal to the analytical quasi-static derivatives (see Ref. 10). This may be one cause for differences between the analytical and identified derivatives. Although engineering judgment cannot be used to assess the validity of each of the sixty derivative estimates, the sign and relative magnitudes of most of the major derivatives can be subjectively analyzed. The major derivative estimates for a pulse and doublet control input are tabulated in Table XIV. From engineering experience (Ref. 11 and 12) it is known that X_u should be negative since it is a direct function of the negative of drag coefficient and should be small, Z_w should be negative and of moderate value since it is a strong function of the negative of lift curve slope. M_w should be negative if the vehicle has longitudinal static stability, but since the rotor is destabilizing M_w may be positive at low speeds until the horizontal tail becomes effective. $M_{\dot{w}}$ should be small and positive for an articulated rotor helicopter and M_q should be negative since all helicopters are known to have pitch damping. N_v should be positive indicating directional static stability and N_r should be negative since yaw damping is present. L_p should be negative and fairly large since the large rotor provides good

roll damping. For the sign convention used the major control derivatives $M_{B_{1s}}$ and $Z_{\theta_{MR}}$ should be negative and $N_{\theta_{TR}}$ and $L_{A_{1s}}$ should be positive, with $L_{A_{1s}}$ substantially greater than $M_{B_{1s}}$ since the same control moment is available for rolling and pitching while there is a large difference in inertias. In addition, since the equations of motion for this investigation include inertial effects in the derivatives Y_r should be approximately equal to minus forward velocity and Z_q should be approximately equal to forward velocity. Examination of Table XIV shows that the identified derivatives comply with all the intuitive tests except M_u, which should be positive for both runs. Analytically predicted derivative estimates are shown along with the complete set of identified deri atives in Tables XV and XVI. The major identified derivatives compare reasonably well with the analytical derivatives but in general predict lower damping derivatives. In addition, the analytical program predicts a positive M_u as would be expected. The non-major derivative values are not intuitively known and the large variation in their estimates between data runs indicates a poor capability to predict these values. Table XVII presents RMS errors between regenerated data and simulated data, as compared to filtered flight data. Figures 6 and 7 contain the regenerated time histories for pulse and doublet inputs, respectively. The simulated time histories for pulse input data simulated by doublet input identified derivatives and vice versa are shown in Figure 8 and 9. The regenerated and simulated time histories all diverge as a function of time, this is due to the unstable eigenvalues of the identified vehicle (see Ref. 2) combined with the presence of process noise. The time history error

equation has the same eigenvalues as the identified vehicle and thus even if the derivative estimates are correct, the time histories will diverge. For the time histories generated in this study the regeneration and simulations were all forced to reinitialize at the filtered data values after each four seconds of flight data. As expected, the correlation between regenerated data and flight data used in the identification process is better than the correlation between simulated data and flight data not used in the identification process. The pulse input data estimates appear to be superior when examining only the regenerated results; however, the more stringent requirement of data simulation verifies the previous result that the doublet input provides the best identifiability. The derivative uncertainties (1 σ) of the major derivatives are shown in Table XVIII for both data runs. Predicted uncertainties for both data runs are relatively small with the doublet input run having slightly lower uncertainties. The high uncertainty associated with M_u for the pulse run is consistent with engineering experience that M_u should be positive. For the doublet input run the uncertainty of M_u is very small and yet the estimate for M_u was also negative. A low predicted uncertainty is therefore not considered to be a sufficient condition for derivative estimate acceptance. However, the uncertainty can be useful in determining whether or not enough data has been processed for derivative convergence or if the controls have sufficiently excited the vehicle to allow identifiability of control derivatives. An examination of Figure 10 shows that the M_u estimate would be in doubt due to its convergence characteristics as compared to the Z_w estimate shown in the same figure.

A comparison of characteristic equation solution (eigenvalues) for the identified derivatives and analytical results is shown in Figure 11. The analytical and identified derivative eigenvalues had similar results consisting of three complex pairs and two aperiodic values. The results of Figure 11 are what would be expected from a classical fixed wing vehicle analysis with three stable complex pairs and one stable aperiodic mode. Helicopters normally exhibit an unstable phugoid oscillation. The identified doublet input derivatives provide the expected helicopter results while the pulse input data results in two unstable oscillations and the analytical program predicts a slightly stable aperiodic mode.

CONCLUSIONS

1. The digital filter cutoff and termination frequencies do not have a major effect on the derivative identification process used for this study below frequences of 4 hz and 5 hz, respectively.

2. The Least Squares Variance Factor (LSQVF) had an appreciable effect on the derivative identification results.

3. The major derivatives identified agreed fairly well with analytical predictions and complied with engineering judgment with the exception of M_u.

4. The predicted uncertainty was not a reliable method for evaluating derivative acceptance but an examination of the time history of estimated uncertainty proved to be useful in determining the adequacy of data content for acceptable derivative identification.

5. The derivative process used in this investigation was fairly sensitive to initial derivative estimates.

6. The derivative process used did not produce consistent values for non-major (off diagonal) derivatives.

7. Flight data regeneration using identified derivatives should be supplemented by flight data simulation when analyzing identified derivative acceptance.

8. Doublet control inputs provide a better data set for identification than pulse or step inputs.

REFERENCES

1. Smetana, F. W.; Delbert, S. C.; and Johnson, D. W.: "Flight Testing Techniques for the Evaluation of Light Aircraft Stability Derivatives - A Review and Analysis." NASA CR-2016, 1972.

2. Molusis, J. A.: "Analytical Study to Define a Helicopter Stability Derivative Extraction Method." NASA CR-132371, May 1973.

3. Gould, D. G. and Hindson, W. S.: "Estimates of the Stability Derivatives of a Helicopter and a V/STOL Aircraft from Flight Data." AGARD Conference Proceedings No. 172 on "Methods for Aircraft State and Parameter Identification." November 1974.

4. Tomaine, R. L.: "Helicopter Parameter Identification Utilizing an Advanced Statistical Algorithm." "Proceedings of the 1975 Army Numerical Analysis and Computers Conference", ARO Report 75-3, February 1975.

5. Graham, R. J.: "Determination and Analysis of Numerical Smoothing Weights." NASA TR-R-179, December 1963.

6. Legacqz, V. J.: "The Efficient Application of Digital Identification Techniques to Flight Data from a Variable Stability V/STOL Aircraft." AGARD Conference Proceedings No. 172 on "Methods for Aircraft State and Parameter Identification." November 1974.

7. Davis, J. M. etal: "Rotorcraft Flight Simulation with Aeroelastic Rotor and Improved Aerodynamic Representation." USAAMRDL TR 74-10A-D, June 1974.

8. Chen, R. T. N.: "Input Design for Aircraft Parameter Identification: Using Time-Optional Control Formulation." AGARD Conference Proceedings No. 172 on "Methods for Aircraft State and Parameter Identification." November 1974.

9. Mehra, R. K. and Gupta, N. K.: "Status of Input Design for Aircraft Parameter Identification." AGARD Conference Proceedings No. 172 on "Methods for Aircraft State and Parameter Identification." November 1974.

10. Molusis, J. A. and Hull, W. E. Jr.: "Rotorcraft Derivative Identification from Analytical Models and Flight Test Data." AGARD Conference Proceedings No. 172 on "Methods for Aircraft State and Parameter Identification." November 1974.

11. Anon.: "Dynamics of the Airframe." Bureau of Aeronautics, Navy Department, Report AE-61-411, September 1952.

12. Gessow, Alfred and Meyers, G. C.: "Aerodynamics of the Helicopter." Frederick Ungov Publishing Co., pp 268-306, New York, N.Y., copywright 1952.

TABLE I.- DESCRIPTION OF TEST VEHICLE

Fusgelage:	Gross Weight N(lbs)	128998.	(29000.)
	I_{xx} Kg-m^2 (slug-ft^2)	39765.	(29329.)
	I_{yy} Kg-m^2 (slug-ft^2)	20364.	(150198.)
	I_{zz} Kg-m^2 (slug-ft^2)	177611.	(130999.)
	I_{xz} Kg-m^2 (slug-ft^2)	-18168.	(-13400.)*
	Length m(ft)	21.41	(70.24)
Main Rotor:	Number of Blades	6	
	Diameter m, (ft)	22.02	(72.26)
	Airfoil	NACA 0010.91	
	Chord cm (in)	60.07	(23.65)
	Total Blade Area m^2(ft^2)	32.72	(352.20)
	Disc Area m^2(ft^2)	378.30	(4072.00)
	Solidity Ratio	.1021	
	Blade Twist (deg)	-7.2000	
	Shaft Tilt-Longitudinal (deg)	3	
	Shaft Tilt-Lateral (deg)	3	
Tail Rotor:	Number of Blades	4	
	Diameter m(ft)	4.88	(16.00)
	Airfoil	NACA 0012	
	Chord cm(in)	38.99	(15.35)
	Total Blade Area m^2(ft^2)	3.08	(33.12)
	Disc Area m^2(ft^2)	18.68	(201.10)
	Solidity Ratio	.198	
	Blade Twist (deg)	-8.000	

TABLE I.- DESCRIPTION OF TEST VEHICLE

(continued)

Horizontal: Stabilizer	Area m^2 (ft^2)	3.72		(40.00)
	Aspect Ratio		1.805	
	Taper Ratio		1.0	
	Incidence Angle (deg)		0.	
	Dihedral Angle (deg)		0.	
Vertical: Fin	Area m^2 (ft^2)	1.55		(16.70)
	Aspect Ratio		5.34	
	Taper Ratio		.733	
	Incidence Angle (deg)		0.	
	Dihedral Angle (deg)		0.	

*Assumed zero for identification process.

TABLE II.- DATA RUN SUMMARY

Flight	Data Run	Airspeed (IAS)	Control Input Shape
38A	1	0 m/sec (hover*)	Doublet
38A	4	152 m/sec (90 Knots)	Doublet
38A	5	101 m/sec (60 Knots)	Pulse
38A	6	101 m/sec (60 Knots)	Step
38B	2	51 m/sec (30 Knots)	Doublet
38B	4	101 m/sec (60 Knots)	Doublet

*Out of ground effect.

All 1G Level Flight

TABLE III.- REGENERATION RMS ERRORS FOR FOUR DIGITAL FILTER FREQUENCIES

Digital Filter f_c/f_t	1/2	2/3	3/4	4/5
Attitudes (deg)	.825	.768	1.370	.750
Velocities m/s (ft/s)	.234 (.767)	.236 (.773)	.237 (.777)	.230 (.754)
Angular Rates (deg/s)	.752	.765	.840	.794
Linear Acc. m/s^2 (ft/s^2)	.273 (.895)	.276 (.907)	.292 (.959)	.281 (.922)
Angular Acc. (deg/s^2)	2.170	2.350	2.040	2.680

TABLE IV.- DERIVATIVE VALUES FOR FOUR DIGITAL FILTER FREQUENCIES

LSQVF = 100

Digital Filter f_c/f_t	1/2	2/3	3/4	4/5
X_u	.04990	-.043400	-.095200	-.01630
M_u^u	.00140	-.000035	-.000549	.00198
L_v	-.00405	-.002570	-.003040	-.00387
N_v^v	.00560	.006640	.006350	.00552
Z_w	-.32700	-.428000	-.224000	-.57900
M_w^w	.00134	-.000500	-.000430	.00434
L_p	-.65600	-.755000	-.607000	-.28100
N_p^p	.15700	.152000	.200000	.38700
Z_q	92.10000	89.300000	80.930000	110.80000
M_q^q	-.27100	-.301000	-.210000	-.68700
L_r	-1.15000	-2.040000	-1.790000	-1.91500
N_r^r	-.65800	-1.020000	-.913000	-1.00000
$M_{B_{1s}}$	-.04090	-.039000	-.030000	-.03760
$L_{A_{1s}}$	.32400	.333000	.317000	.27600
$N_{\theta_{TR}}$	.07300	.058000	.059000	.06830
$Z_{\theta_{MR}}$	-2.14000	-2.800000	-3.200000	-3.05000

TABLE V.- MAJOR DERIVATIVE UNCERTAINTY FOR FOUR DIGITAL FILTER FREQUENCIES

Digital Filter f_c/f_t	Uncertainty % 1/2	2/3	3/4	4/5
X_u	42.5	87.0	13.1	159.0
M_u	40.0	34.8	129.0	26.1
L_v	40.2	47.8	11.0	24.9
N_v	11.4	10.9	6.2	7.4
Z_w	9.6	9.5	3.4	7.7
M_w	3.3	18.0	32.4	10.7
L_p	15.2	15.6	7.4	20.9
N_p	24.6	16.2	6.2	8.0
Z_q	5.5	6.5	2.7	6.0
M_q	22.5	18.6	26.0	11.3
L_r	18.5	12.8	5.7	6.9
N_r	14.0	11.4	6.3	6.5
$M_{B_{is}}$	7.6	7.6	5.1	6.9
$L_{A_{is}}$	5.0	4.3	2.0	3.0
N_{TR}	6.8	7.0	3.5	4.5
Z_{MR}	10.4	10.9	3.8	7.4

TABLE VI.- REGENERATION RMS ERRORS FOR FIVE VALUES OF LSQVF

RMS \ LSQVF	25	50	75	100	150
Attitudes (deg)	1.89	.938	2.162	1.370	.892
Velocities (ft/s)	1.76	.791	2.375	.777	.798
A. Vel. (deg/s)	1.18	.852	1.368	.840	.848
Linear Acc. (ft/s)	1.55	.973	1.697	.959	.956
Ang Acc. (deg/s)	2.84	2.710	2.984	2.040	2.740
AVG	1.844	1.253	2.117	1.197	1.247

TABLE VII.- DERIVATIVE VALUES FOR FIVE VALUES OF LSQVF

LSQVF	25	50	75	100	150
X_u	-.08360	-.070300	118100	-.090000	-.101300
M_u	-.00211	-.000413	-.000225	-.000293	-.000130
L_v	-.00497	-.005830	-.005000	-.005620	-.005160
N_v	.005330	.005410	.005320	.005330	.005390
Z_w	-.39300	-.642000	-.462000	-.718000	-.777000
M_w	-.00120	.001160	.001160	.001180	.000996
L_p	-.54900	-.511000	-.515000	-.509000	-.543000
N_p	.23600	.274000	.240000	.278000	.265000
Z_q	91.20000	94.100000	96.900000	97.490000	99.770000
M_q	-.14500	-.141000	-.168000	-.144000	-.131000
L_r	-1.39000	-1.387000	-1.290000	-1.350000	-1.370000
N_r	-.74400	-.731000	-.679000	-.695000	-.664000
$M_{B_{1s}}$	-.03900	-.036600	-.042100	-.037200	-.036700
$L_{A_{1s}}$	.30300	.300000	.294000	.296000	.295000
$N_{\theta_{TR}}$	.07010	.071300	.070500	.070200	.070100
$Z_{\theta_{MR}}$	-.86600	-2.970000	-.818000	-3.130000	-3.260000

TABLE VIII.- DERIVATIVE UNCERTAINTIES
FOR FIVE VALUES OF LSQVF

Uncertainty %

LSQVF	25	50	75	100	150
X_u	12.6	15.8	10.0	13.1	12.8
M_u^u	168.0	87.8	175.0	129.0	318.0
L_v	12.5	10.5	12.7	11.0	12.7
N_v^v	6.3	6.0	6.5	6.2	6.4
Z_w	4.8	3.4	4.5	3.4	3.3
M_w^w	28.8	31.4	31.5	32.4	40.0
L_p	6.8	7.2	7.3	7.4	7.1
N_p^p	7.2	6.3	7.2	6.2	6.6
Z_q	2.4	2.6	2.5	2.7	2.8
M_q^q	24.2	26.0	22.2	26.0	29.5
L_r	5.6	5.6	6.0	5.7	5.8
N_r^r	5.9	6.0	6.5	6.3	6.5
$M_{B_{IS}}$	4.7	5.1	4.6	5.1	5.2
$L_{A_{IS}}$	1.9	2.0	2.0	2.0	2.1
$N_{e_{TR}}$	2.8	3.4	2.9	3.5	3.5
$Z_{e_{MR}}$	6.5	3.8	7.3	3.8	3.8

TABLE IX.- EFFECT OF INITIAL DERIVATIVE ESTIMATE ON IDENTIFIED DERIVATIVES

Original Identified Derv.		Identified Derv. with 50% Increase in Initial Estimate	% Difference
X_u	-.095200	-.11080	+16.4
M_u	-.000549	-.00044	-19.9
L_v	-.003040	-.00620	104.0
N_v	-.006350	.00515	-18.9
Z_w	-.224000	-.87100	+289.0
M_w	-.000430	.00150	+449.0
L_p	-.607000	-.50400	-17.0
N_p	.200000	.30000	+5 .0
Z_q	80.930000	105.60000	+30.5
M_q	-.210000	-.16400	-21.9
L_r	-1.790000	-1.38000	-22.9
N_r	-.913000	-.73800	-19.2
$M_{B_{1s}}$	-.030000	-.03700	+23.3
$L_{A_{1s}}$	.317000	.29300	-7.6
$N_{\theta_{TR}}$	.059000	.06990	+18.5
$Z_{\theta_{MR}}$	-3.200000	-3.72000	+16.3

TABLE X.- IDENTIFIED DERIVATIVE VALUES FOR THREE CONTROL INPUT SHAPES

Digital Filter = 1/2 LSQVF = 62.5

Input	Pulse	Doublet	Step
X_u	-.030200	-.25560	-.98500
M^u_u	.000027	-.00235	.00086
L_v	-.001980	-.00454	-.00139
N^v_v	.007180	.00347	.00356
Z_w	-.374000	-.41600	2.13500
M^w_w	-.001170	-.00048	.00331
L_p	-.769000	-.71700	-.60800
N^p_p	.117000	.08080	-.03050
Z_q	87.860000	108.10000	-444.60000
M^q_q	-.239000	-.75800	-.94200
L_r	-1.740000	-.10400	-.62600
N^r_r	-.861000	-.79800	-.33200
$M_{B_{1s}}$	-.038300	-.04390	-.01750
$L_{A_{1s}}$	.335000	.07700	.18900
$N_{\theta_{TR}}$	.057300	.05870	.03880
$Z_{\theta_{TR}}$	-2.720000	-2.75900	15.18000

TABLE XI.- DERIVATIVE UNCERTAINTIES FOR THREE CONTROL INPUT SHAPES

Input Shape	Uncertainty % 38A5 Pulse	38B4 Doublet	38A6 Step
X_u	53.8	8.1	2.6
M_u^u	1276.0	17.0	8.0
L_v	9.8	11.6	31.5
N_v^v	9.4	8.5	5.4
Z_w	1263.0	5.0	1.7
M_w^w	51.0	52.1	6.5
L_p	13.5	11.0	8.8
N_p^p	34.0	42.0	63.0
Z_q	5.8	3.7	1.9
M_q^q	24.0	6.5	5.3
L_r	12.8	67.9	10.7
N_r^r	11.4	6.5	9.5
$M_{B_{1s}}$	8.23	3.8	68.0
$L_{A_{1s}}$	5.1	9.1	4.8
$N_{\theta_{TR}}$	8.4	4.0	4.9
$Z_{\theta_{MR}}$	7.8	5.1	1.4

TABLE XII.- RMS REGENERATION AND SIMULATION ERRORS FOR THREE CONTROL INPUT SHAPES

Flight Data ↓ from ⟶ Identified Derivatives

Input Shape		38A-5 Pulse		38B-4 Doublet		38A-6 Step	
38A-5 Pulse	Att.	6.20		1.260		4.910	
	Vel.	6.41		1.858		13.570	
	Rates	4.50	R	1.170	S	6.840	S
	L. Acc.	4.37		1.974		16.680	
	A. Acc.	4.67		1.940		3.750	
	Avg.	5.07		1.628		8.247	
38B-4 Doublet	Att.	15.10		4.774		12.860	
	Vel.	14.78		6.319		85.100	
	Rates	8.63	S	2.641	R	11.810	S
	L. Acc.	10.43		3.483		45.370	
	A. Acc.	9.22		2.766		8.400	
	Avg.	11.34		3.766		29.390	
38A-6 Step	Att.	13.94		8.740		41.600	
	Vel.	14.50		9.190		136.500	
	Rates	9.04	S	4.170	S	29.500	R
	L. Acc.	10.23		6.075		114.000	
	A. Acc.	8.84		3.890		16.900	
	Avg.	11.14		6.260		62.000	

R - Regeneration

S - Simulation

Digital Filter = 1/2

LSQVF = 62.5

TABLE XIII.- EFFECT OF AIRSPEED ON DERIVATIVE VALUES

Derivative	Airspeed (IAS)			
	0 m/sec (Hover)	52 m/sec (30 Knots)	101 m/sec (60 Knots)	152 m/sec (90 Knots)
X_u	-.07880 -.01890	.242000 -.026000	-.030200 -.046400	.053600 -.069900
M_u	.00805 .00179	.004600 .001210	.000270 .000943	.001400 .001320
L_v	-.04610 -.03490	.000287 -.028700	.001980 -.020900	-.005800 -.014400
N_v	-.00807 .04100	.00217 .03980	-.007180 .033500	.004020 .026200
Z_w	.12600 -.35900	-.10400 -.56400	-.374000 -.800000	.734000 -.949700
M_w	-.00249 -.00154	.00295 -.00150	-.001170 -.001080	-.004200 -.000808
L_p	-.88000 -2.19500	-.48100 -2.22400	-.769000 -1.992000	-.361000 -1.629000
N_p	-.24600 1.10400	-.29100 .90200	-.117000 .481000	.008600 -.001960
Z_q	-4.08000 1.35300	29.30000 51.39500	87.860000 100.650000	127.300000 150.020000
M_q	-.15500 -.42700	-1.03000 -.41400	-.239000 -.471000	-.149000 -.518000
L_r	.41500 .20400	.32400 .29400	-1.740000 .377000	-.134000 .613000
N_r	.07020 -.36500	-.35700 -.47500	-.861000 -.664000	-.794000 -1.036000
$M_{B_{1s}}$	-.03560 -.11240	-.02870 -.11070	-.030300 -.110900	-.040800 -.114600
$L_{A_{1s}}$	.37500 .38100	.18100 .37700	.335000 .375000	.329000 .382000
$N_{\theta_{TR}}$	.03630 .09910	.03350 .10090	.057300 .122600	.074700 .143000
$Z_{\theta_{MR}}$	-2.51000 -5.64600	-3.23000 -5.49300	-2.720000 -6.494000	-2.900000 -7.615000

1st item identified derivative, 2nd item analytical estimates

TABLE XIV.- MAJ[illegible]DENTIFIED DERIVATIVES
FOR PULSE AND DOUBLET INPUTS

	Pulse Input 38A-5	Doublet Input 38B-4
X_u	-.090000	-1.23000
M_u	-.000293	-.00321
L_v	-.005620	-.00750
N_v	-.005330	.00304
Z_w	-.718000	-.57500
M_w	.001180	-.00099
L_p	-.509000	-.33100
N_p	.278000	.11300
Z_q	97.490000	101.10000
M_q	-.144000	-.72400
L_r	-1.350000	.01660
N_r	-.695000	-.78800
$M_{B_{1s}}$	-.037200	-.04400
$L_{A_{1s}}$	.296000	.23200
$N_{\theta_{TR}}$	.070200	.05800
$Z_{\theta_{MR}}$	-3.130000	-2.86000

Digital Filter = 3/4

LSQVF = 100

A/S $\approx$ [illegible]01 m/sec (60 Knots)

TABLE V.- PULSE INPUT IDENTIFIED DERIVATIVES COMPARED TO ANALYTICAL ESTIMATES (C-81)

	X	Y	Z	L	M	N
u	-.09000 -.04320	-.02980 .07420	.14700 -.08940	-.00965 -.01830	-.000293 .000943	-.00263 .01810
v	.02590 -.00742	.09030 -.24000	-.12500 -.05500	-.00562 -.02090	-.001070 .000946	.00533 .03350
w	.24000 .03960	.29000 -.07250	-.71800 -.74600	-.00860 -.00293	.001180 -.001080	-.00534 .01430
p	-2.86000 -.78700	2.97000 -5.68500	37.00000 -2.66200	-.50900 -1.99200	-.229000 .172000	.27800 .48100
q	8.24600 3.62700	10.10000 -4.71300	97.49000 97.92100	2.80000 -1.62600	-.144000 -.471000	1.05000 1.34300
r	-25.10000 -.34300	-95.59000 -96.33400	-3.99000 3.16200	-1.35000 .37700	-.138000 .037100	-.69500 -.66400
B_{1s}	1.79000 .79900	-.32300 .02400	1.91500 1.97900	.10300 -.04560	-.037200 -.111000	.02060 .01060
A_{1s}	-.24600 .02580	-.00018 .58300	-1.78400 .09240	.29600 .37500	.008410 -.003820	.00873 .00322
θ_{TR}	-.02410 -.02170	-.42800 -.41300	-.09930 -.00923	.04690 -.07380	.002950 -.004020	.07020 .12300
θ_{MR}	1.01000 .081900	-.43100 -.20500	-3.13000 -6.04700	02740 .02520	.009500 .020500	.03010 .08900

Analytical Estimates are Listed Below Identified Derivatives, Run 38A-5, LSQVF = 100, Digital Filter - 3/4.

TABLE XVI.- DOUPLET INPUT IDENTIFIED DERIVATIVES
COMPARED WITH ANALYTICAL ESTIMATES (C-81)

	X	Y	Z	L	M	N
u	-1.23000 -.04320	.51500 -.07420	-.45100 -.08940	-.07980 -.01830	-.003210 .000943	-.00686 .01810
v	-.03970 -.00742	-.06260 -.24000	.05910 -.05500	-.07500 -.02090	.001740 .000946	.00304 .03350
w	-.36800 .03960	.03840 -.07250	-.57500 -.74600	-.02030 -.00293	-.000990 -.001080	-.00648 .01430
p	-16.14000 -.78700	15.47000 -4.25500	34.25000 -2.66200	-.33100 -1.99200	-.030.00 .172000	.11300 .48100
q	21.97000 2.19700	25.40000 -4.71300	101.10000 98.76000	5.45000 -1.62600	-.724000 -.471000	1.12900 1.34300
r	-13.30000 -.34300	-79.53000 -97.19400	10.59000 3.16200	.01660 .37700	-.077800 .037100	-.78800 -.66400
B_{1s}	.09860 .79900	.79900 .02400	.54400 .97900	.06460 -.04560	-.044000 -.111000	.02380 .01060
A_{1s}	3.48000 .02580	-1.39000 .58300	.92600 .09240	.23200 .37500	.010400 -.003820	.01900 .00322
θ_{TR}	.24100 -.02170	.04500 -.41300	-.17300 -.00923	-.02450 -.07380	.003560 -.004020	.05800 .12300
ϵ_{MR}	.01400 .08190	-.00128 -.20500	-2.86000 -6.04700	-.04500 .02520	.009770 .020500	.02470 .08900

Analytical Estimates are Listed Below Identified Derivatives, Run 38B-4,
LSQVF = 100, Digital Filter = 3/4.

TABLE XVII.- REGENERATED AND SIMULATED RMS ERRORS FOR PULSE AND DOUBLET INPUTS

Identified Derivatives ↓	Flight Data →	38A-5 (pulse)	38B-4 (doublet)
Pulse	Attitudes deg.	1.370	3.280
	Velocities m/s (ft/s)	.237 (.777)	1.146 (3.760)
	A. Rates deg/s	.840 R	2.760 S
	Linear Accel. m/s^2 (ft/s^2)	.290 (.952)	.859 (2.820)
	A. Accel. deg/s^2	2.040	2.080
Doublet	Attitudes deg.	1.466	1.745
	Velocities m/s (ft/s)	.610 (2.000)S	.753 (2.470) R
	A. Rates deg/s	1.456	1.450
	Linear Accel. m/s^2 (ft/s^2)	.528 (1.733)	.485 (1.590)
	A. Accel. deg/s^2	3.418	2.137

R - Regenerated

S - Simulation

TABLE XVIII.- MAJOR DERIVATIVE UNCERTAINTIES FOR PULSE AND DOUBLET INPUTS

Derivative	Uncertainty %: Pulse (38A-5)	Uncertainty %: Doublet (38B-4)
X_u	13.1	2.7
M_u^u	129.0	1.9
L_v	11.0	8.4
N_v^v	6.2	6.0
Z_w	3.4	2.8
M_w^w	32.4	25.0
L_p	7.4	14.6
N_p^p	6.2	16.9
Z_q	2.7	2.1
M_q^q	26.0	4.2
L_r	5.7	4.5
N_r^r	6.3	3.5
$M_{B_{1s}}$	5.1	2.3
$L_{A_{1s}}$	2.0	2.5
$N_{\delta_{TR}}$	3.5	2.1
$Z_{\delta_{MR}}$	3.8	2.8

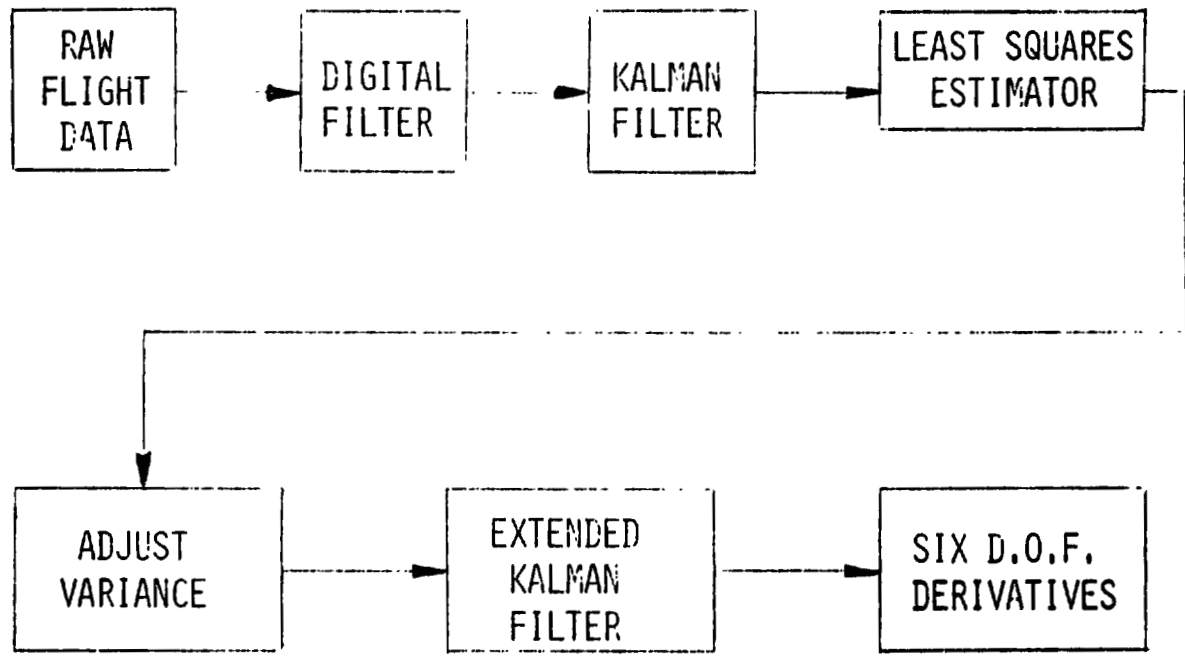

Figure 1.- Schematic of stability derivative extraction process.

$$\dot{u} = \dot{u}_0 - g\sin\theta_0 + \frac{\partial X}{\partial u}u + \frac{\partial X}{\partial v}v + \frac{\partial X}{\partial w}w + \frac{\partial X}{\partial p}p + \left(\frac{\partial X}{\partial q} - w_0\right)q + \frac{X}{r}r + \frac{\partial X}{\partial B_{1s}}\zeta B_{1s} + \frac{\partial X}{\partial A_{1s}}\zeta A_{1s} + \frac{\partial X}{\partial \theta_{TR}}\zeta\theta_{TR} + \frac{\partial X}{\partial \theta_{MR}}\zeta\theta_{MR}$$

$$\dot{v} = \dot{v}_0 + g\sin\phi_0\cos\theta_0 + \frac{\partial Y}{\partial u}u + \frac{\partial Y}{\partial v}v + \frac{\partial Y}{\partial w}w + \left(\frac{\partial Y}{\partial p} + w_0\right)p + \frac{\partial Y}{\partial q}q + \left(\frac{\partial Y}{\partial r} - u_0\right)r + \frac{\partial Y}{\partial B_{1s}}\zeta B_{1s} + \frac{\partial Y}{\partial A_{1s}}\zeta A_{1s} + \frac{\partial Y}{\partial \theta_{TR}}\zeta\theta_{TR} + \frac{\partial X}{\partial \theta_{MR}}\zeta\theta_{MR}$$

$$\dot{w} = \dot{w}_0 + g\cos\phi_0\cos\theta_0 + \frac{\partial Z}{\partial u}u + \frac{\partial Z}{\partial v}v + \frac{\partial Z}{\partial w}w + \frac{\partial Z}{\partial p}p + \left(\frac{\partial Z}{\partial q} + u_0\right)q + \frac{\partial Z}{\partial r}r + \frac{\partial Z}{\partial B_{1s}}\zeta B_{1s} + \frac{\partial Z}{\partial A_{1s}}\zeta A_{1s} + \frac{\partial Z}{\partial \theta_{TR}}\zeta\theta_{TR} + \frac{\partial Z}{\partial \theta_{MR}}\zeta\theta_{MR}$$

$$\dot{p} = \frac{\partial L}{\partial u}u + \frac{\partial L}{\partial v}v + \frac{\partial L}{\partial w}w + \frac{\partial L}{\partial p}p + \frac{\partial L}{\partial q}q + \frac{\partial L}{\partial r}r + \frac{\partial L}{\partial B_{1s}}\zeta B_{1s} + \frac{\partial L}{\partial A_{1s}}\zeta A_{1s} + \frac{\partial L}{\partial \theta_{TR}}\zeta\theta_{TR} + \frac{\partial L}{\partial \theta_{MR}}\zeta\theta_{MR}$$

$$\dot{q} = \frac{\partial M}{\partial u}u + \frac{\partial M}{\partial v}v + \frac{\partial M}{\partial w}w + \frac{\partial M}{\partial p}p + \frac{\partial M}{\partial q}q + \frac{\partial M}{\partial r}r + \frac{\partial M}{\partial B_{1s}}\zeta B_{1s} + \frac{\partial M}{\partial A_{1s}}\zeta A_{1s} + \frac{\partial M}{\partial \theta_{TR}}\zeta\theta_{TR} + \frac{\partial M}{\partial \theta_{MR}}\zeta\theta_{MR}$$

$$\dot{r} = \frac{\partial N}{\partial u}u + \frac{\partial N}{\partial v}v + \frac{\partial N}{\partial w}w + \frac{\partial N}{\partial p}p + \frac{\partial N}{\partial q}q + \frac{\partial N}{\partial r}r + \frac{\partial N}{\partial B_{1s}}\zeta B_{1s} + \frac{\partial N}{\partial A_{1s}}\zeta A_{1s} + \frac{\partial N}{\partial \theta_{TR}}\zeta\theta_{TR} + \frac{\partial N}{\partial \theta_{MR}}\zeta\theta_{MR}$$

$$\dot{\phi} = p + (r\cos\phi + q\sin\phi)\tan\theta$$

$$\dot{\theta} = q\cos\phi - r\sin$$

$$\dot{\psi} = \frac{(r\cos\phi + q\sin\phi)}{\cos\theta}$$

Figure 2.- Equations of motion.

Figure 3. CH-54B test vehicle.

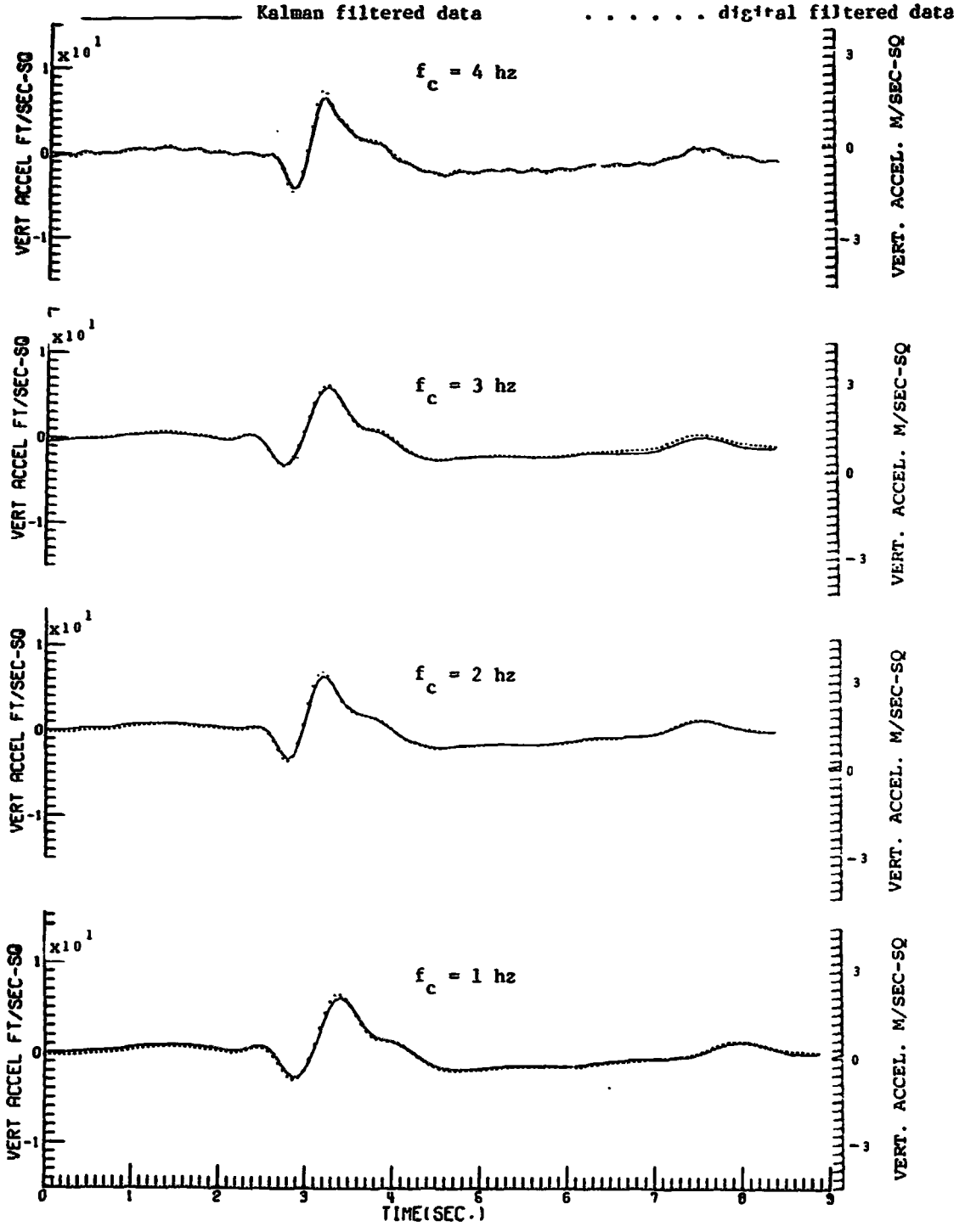

Figure 4.- Effect of digital filter frequency on vertical acceleration measurement.

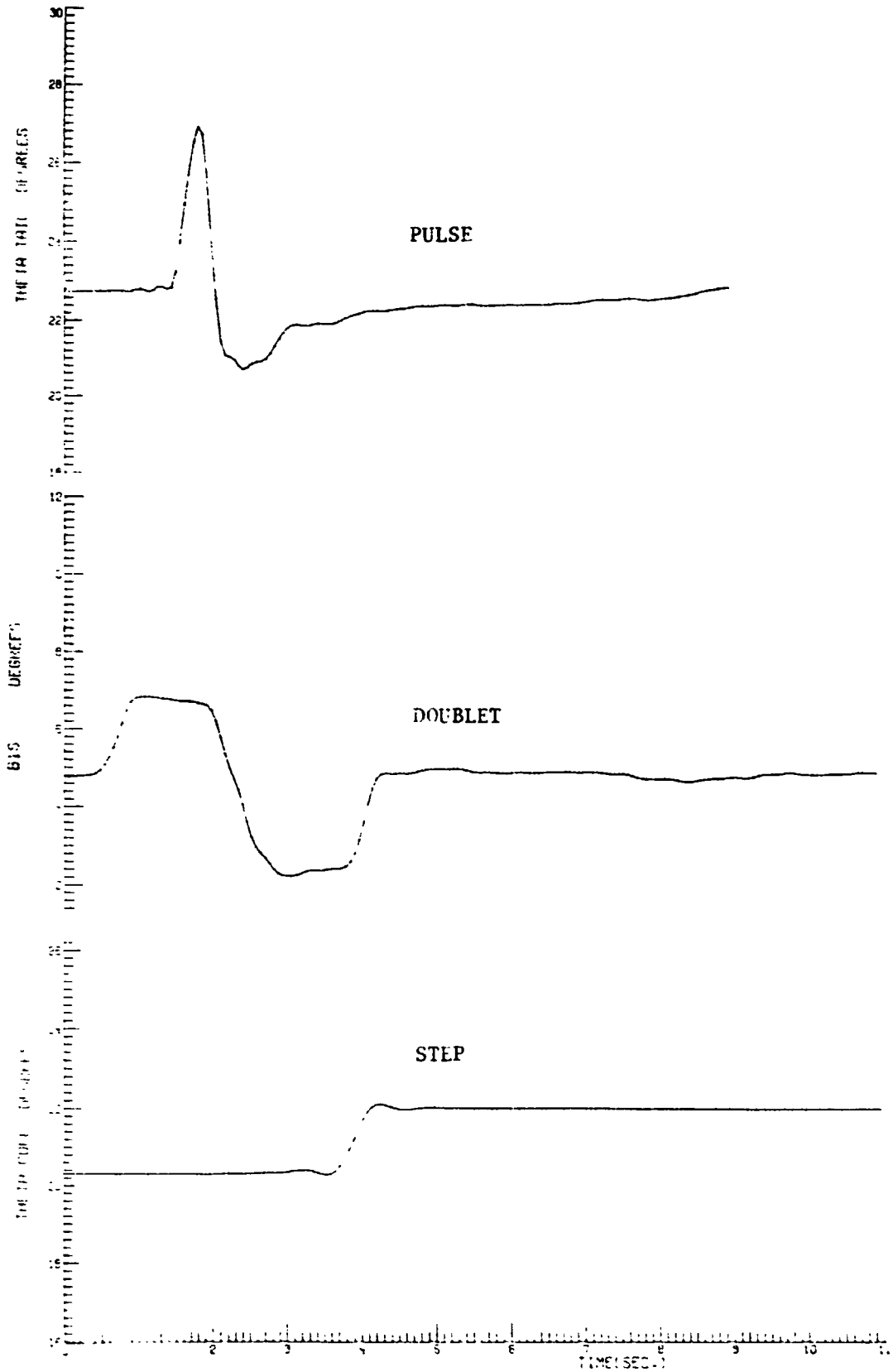

Figure 5.- Representative input shapes.

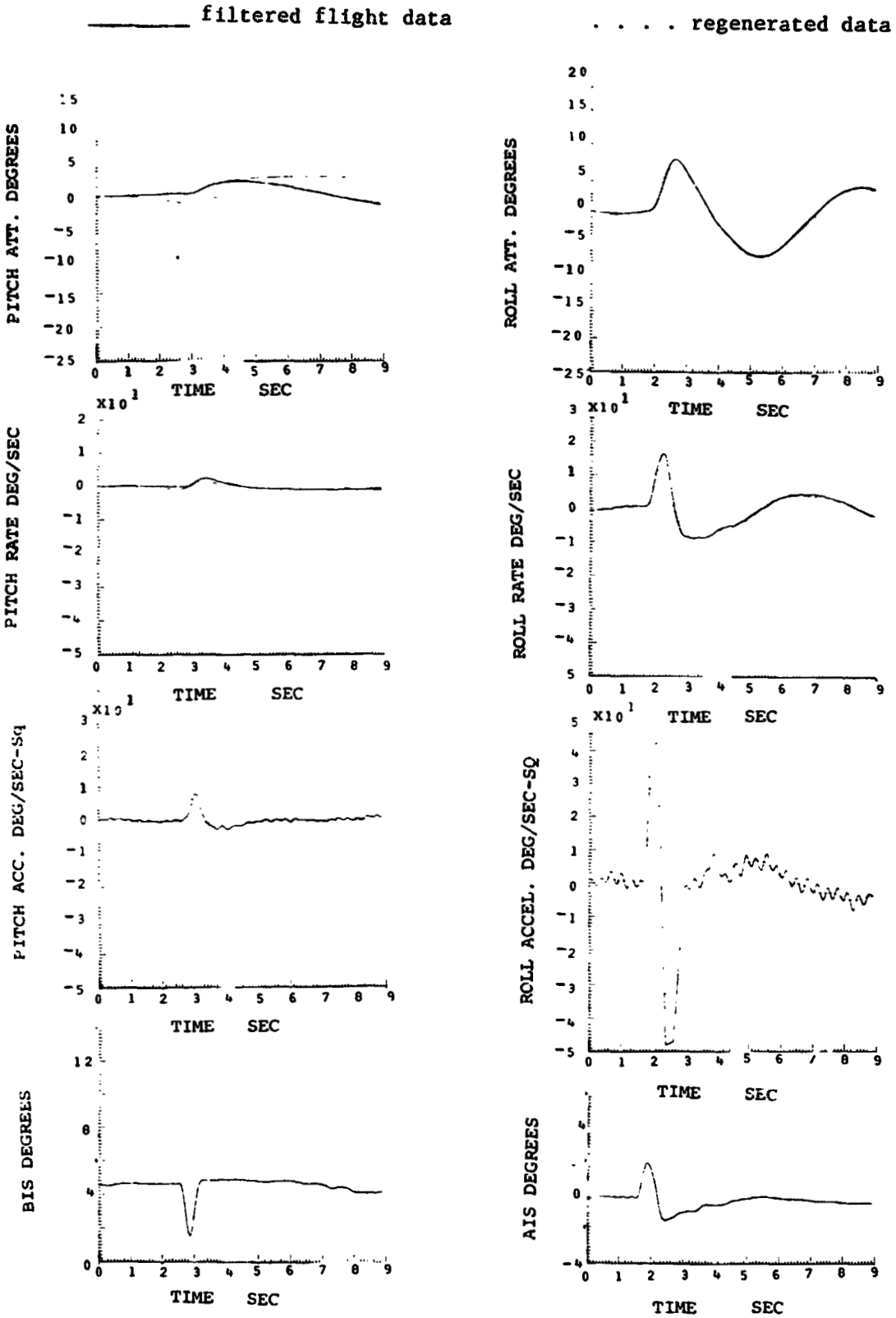

Figure 6.- Pulse input regenerated time histories.

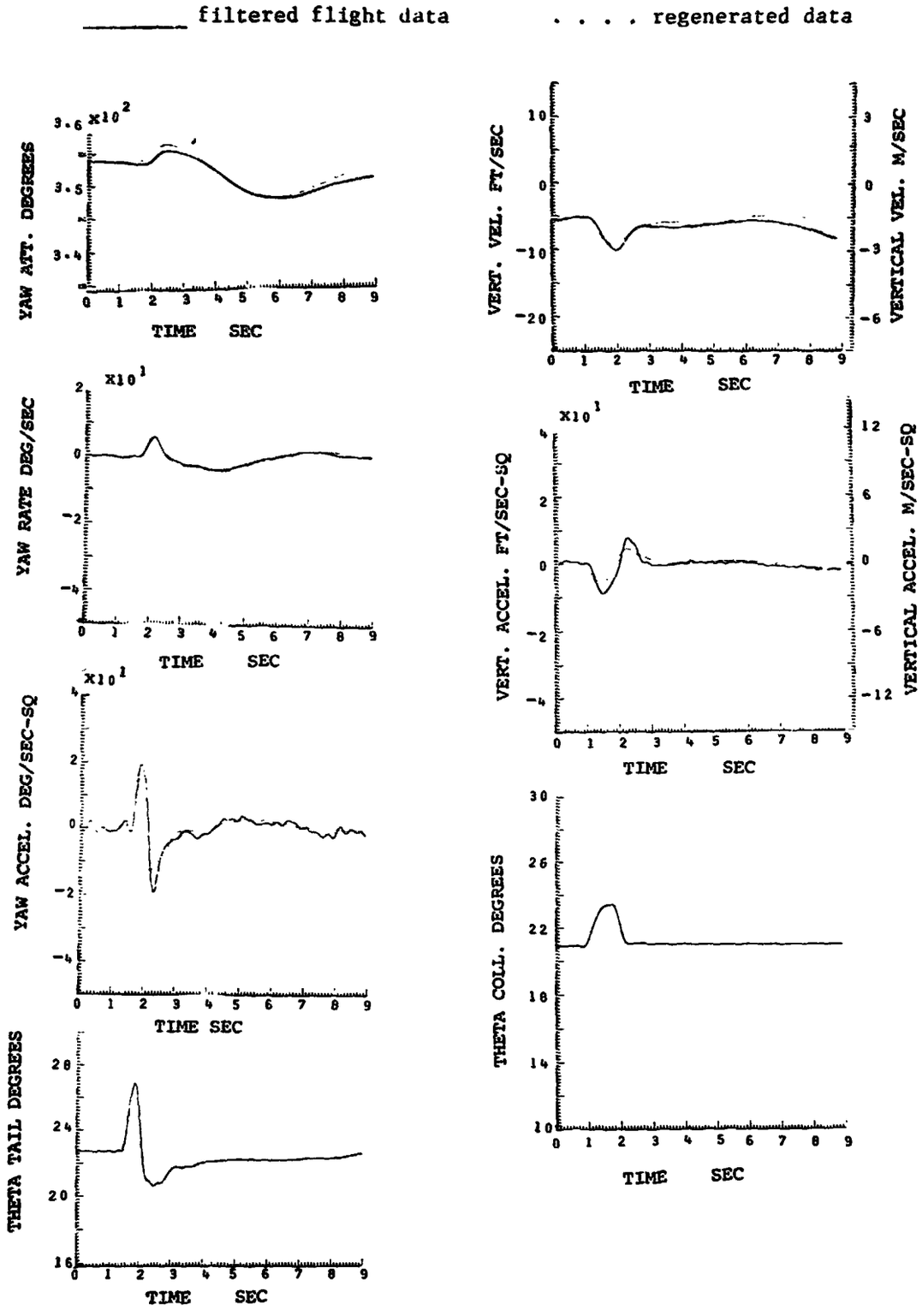

Figure 6.- Concluded.

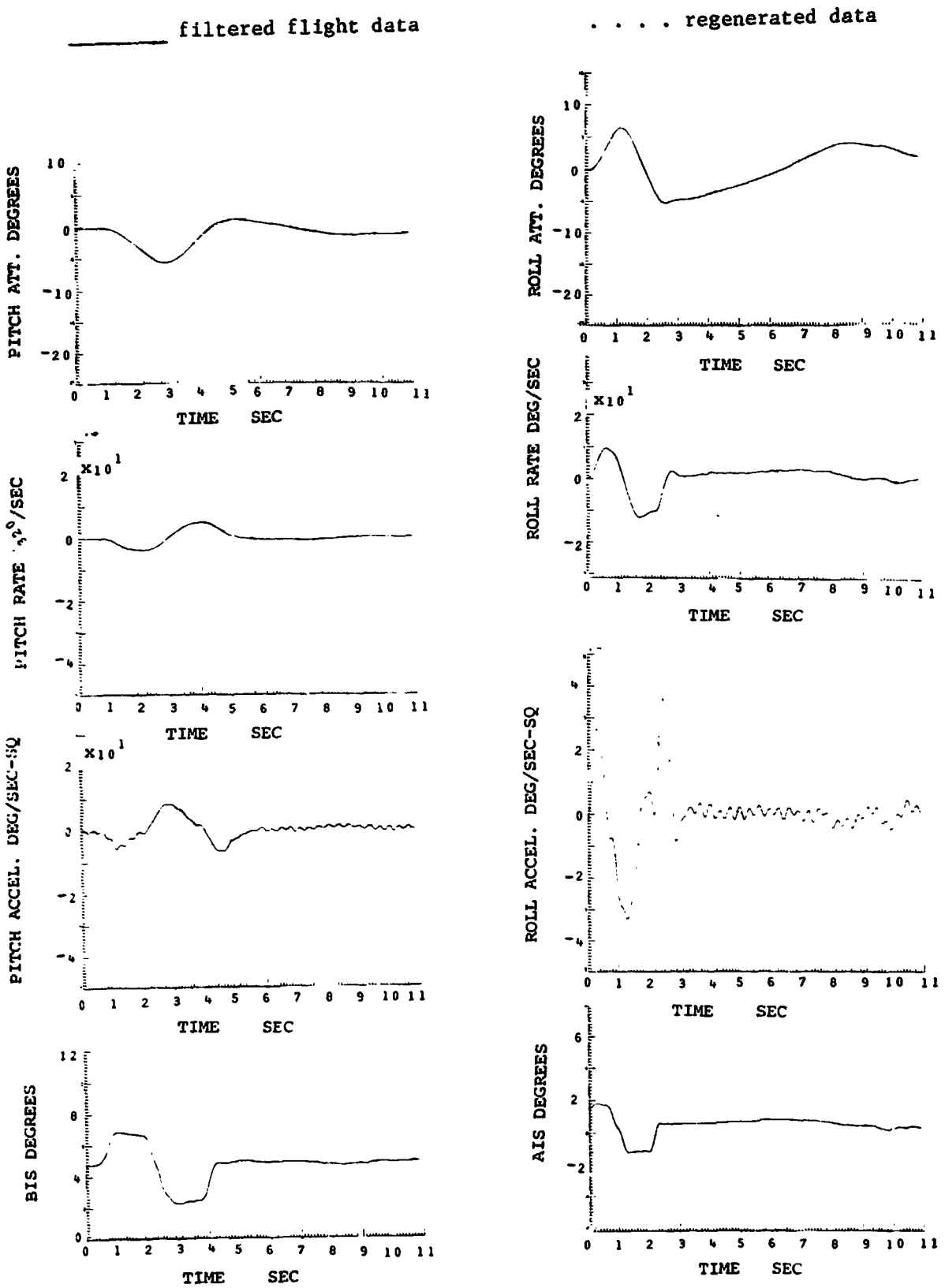

Figure 7.- Doublet input regenerated time histories.

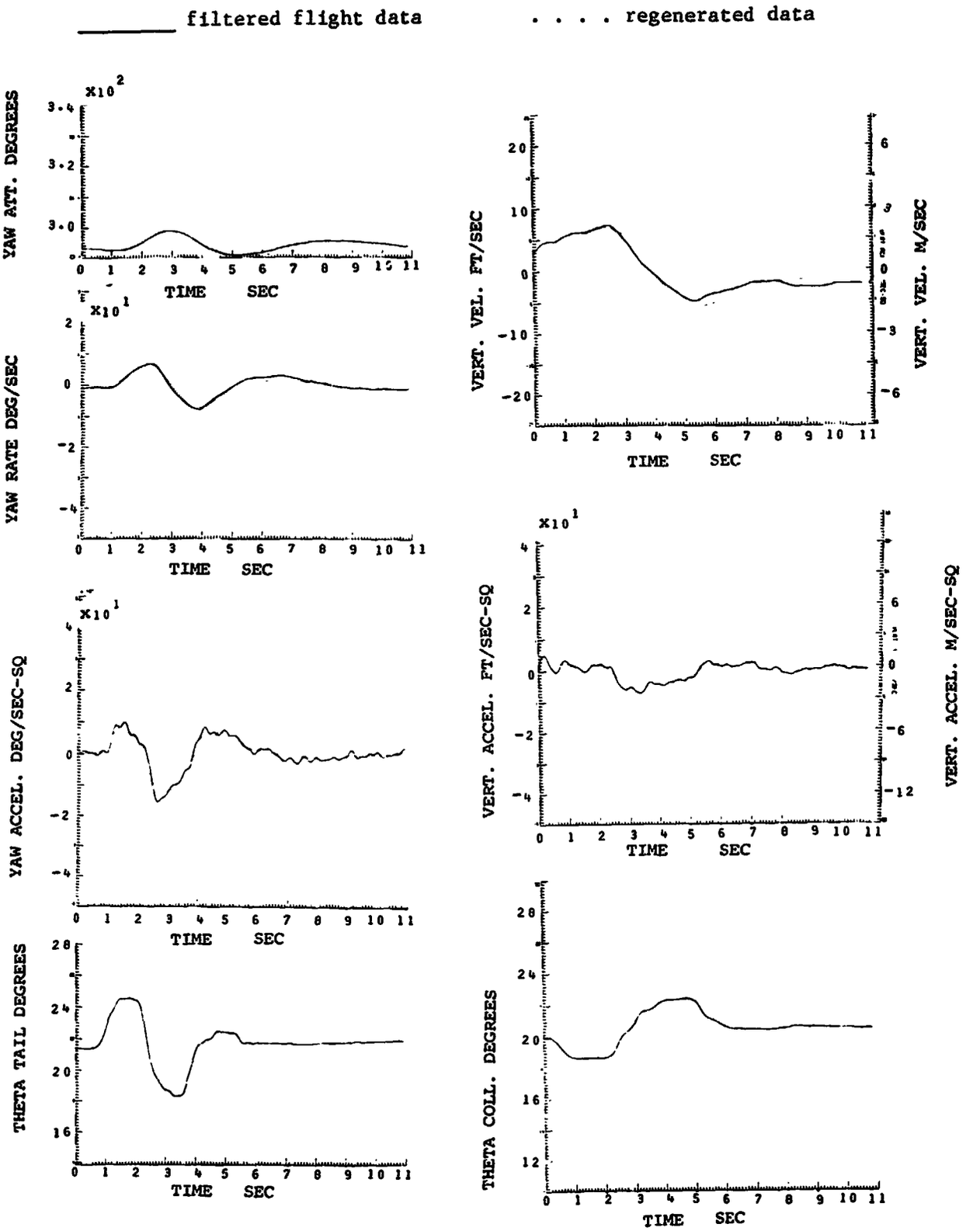

Figure 7.- Concluded

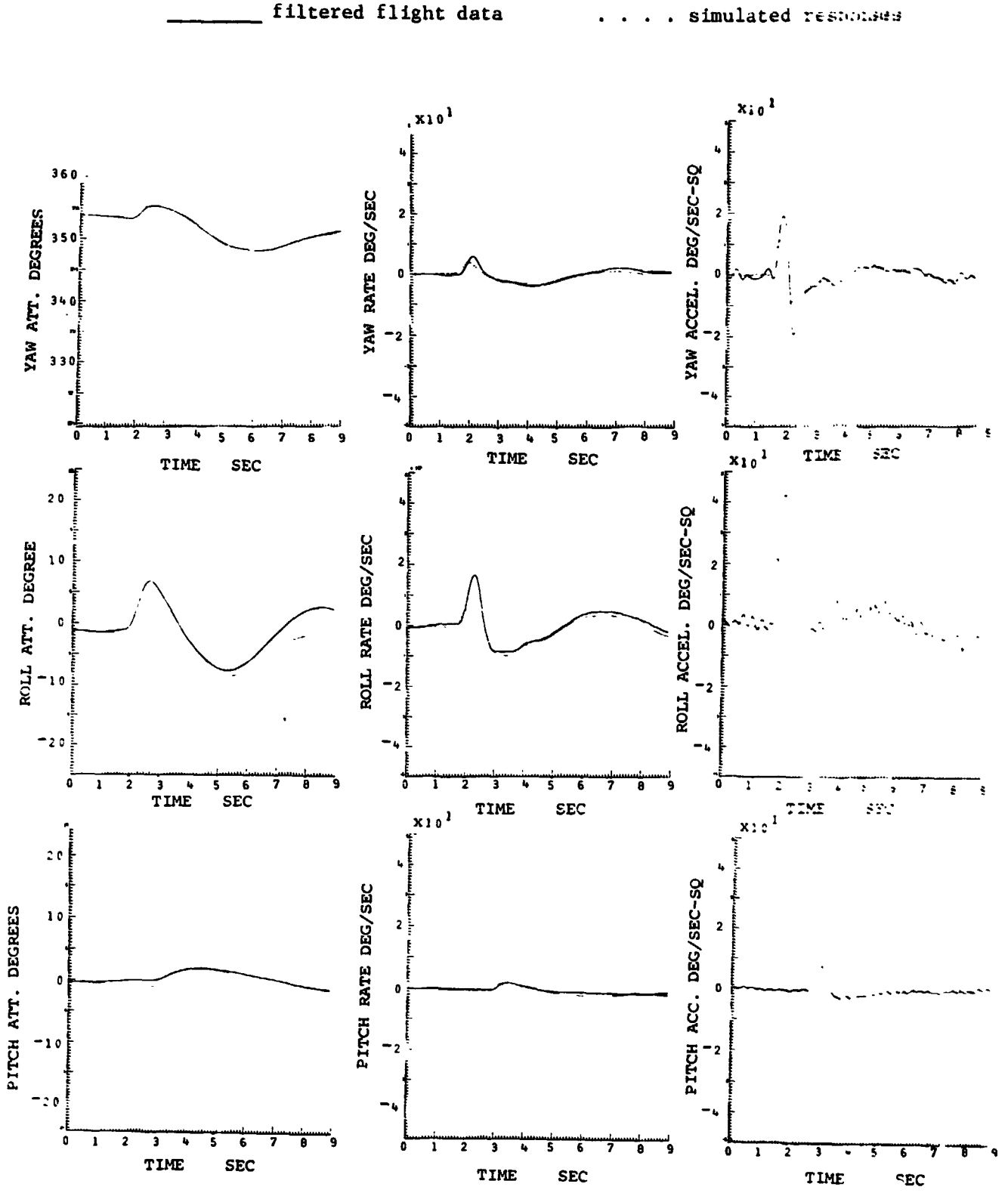

Figure 8.- Pulse input simulated time histories.

filtered flight data . . . . simulated responses

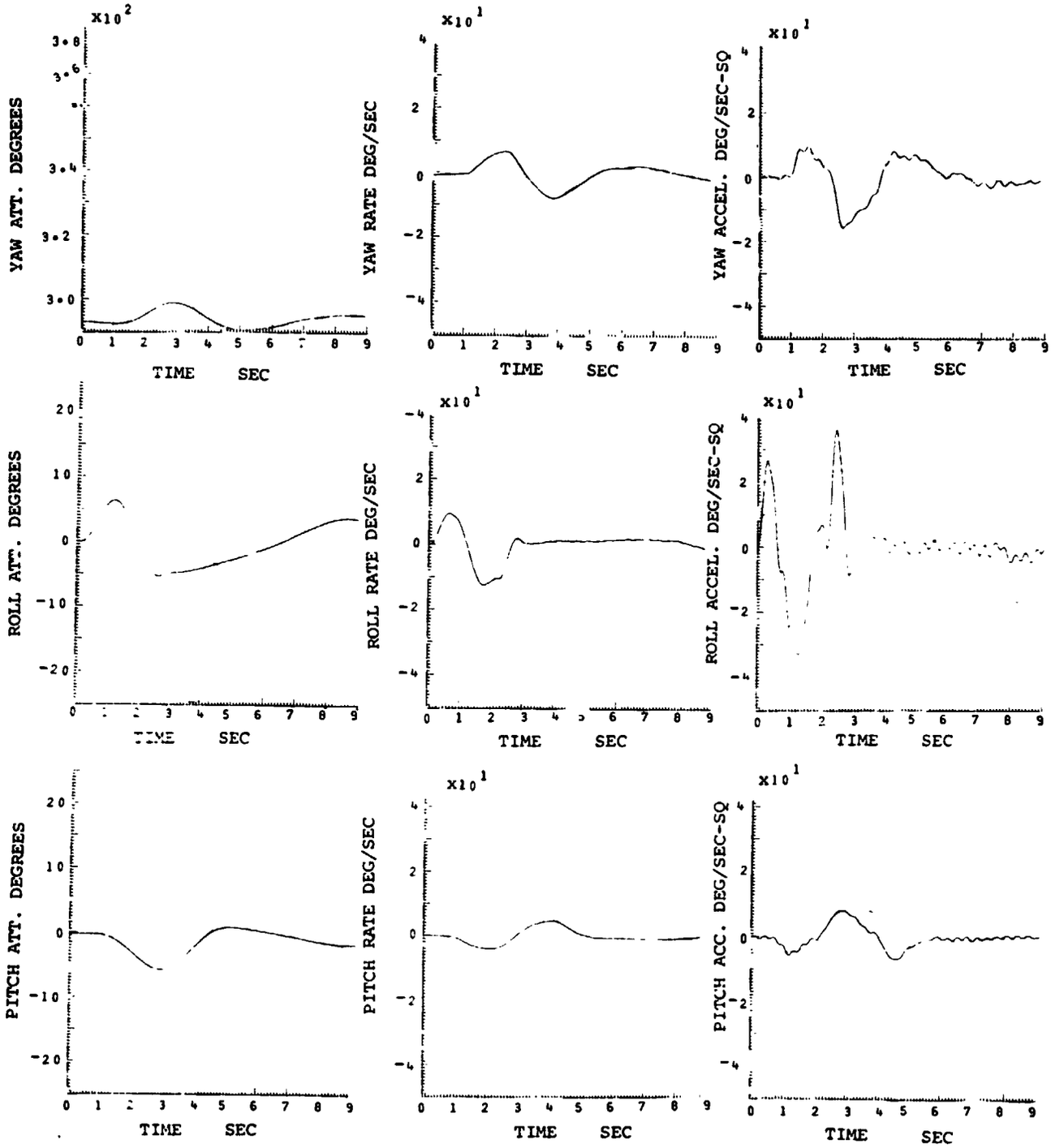

Figure 9.- Doublet input simulated time histories.

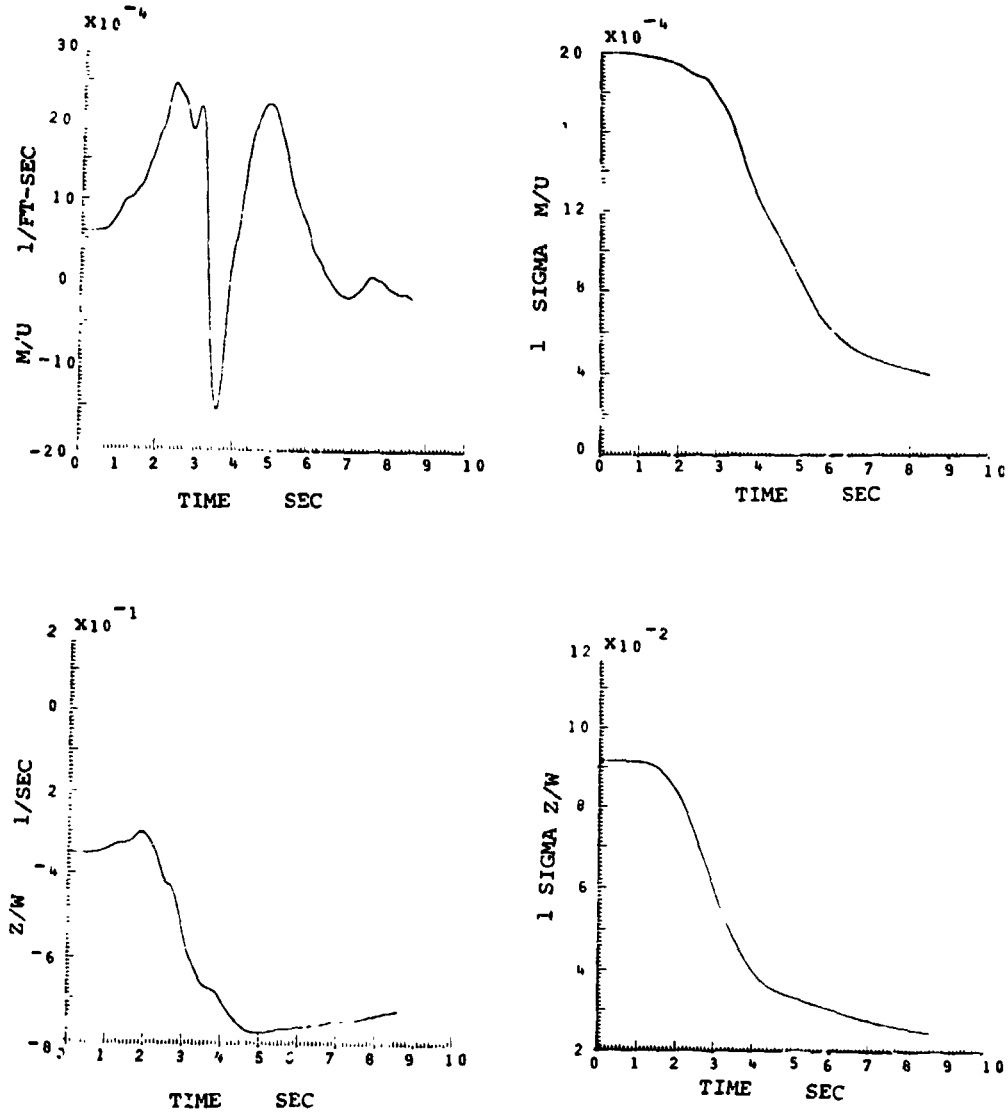

Figure 10.- M_u and Z_w convergence time histories.

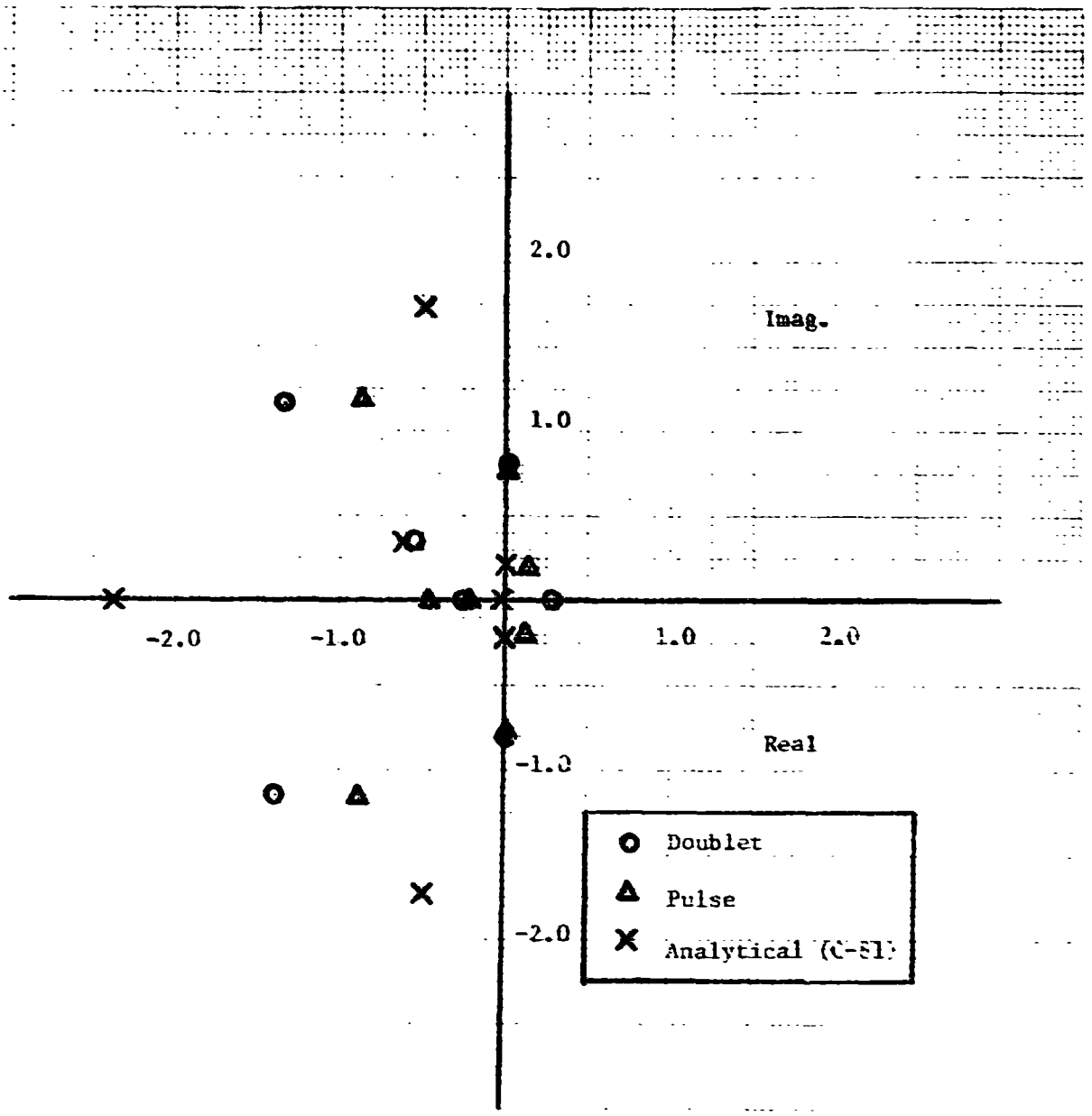

A/S = 101 m/sec (60 knots) Digital Filter = 3/4 LSQVF = 100

Figure 11.- Eigenvalues for identified and analytical derivatives.